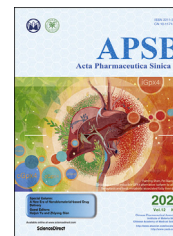




Chinese Pharmaceutical Association  
Institute of Materia Medica, Chinese Academy of Medical Sciences

Acta Pharmaceutica Sinica B

[www.elsevier.com/locate/apsb](http://www.elsevier.com/locate/apsb)  
[www.sciencedirect.com](http://www.sciencedirect.com)



LETTER TO THE EDITOR

# Rapid screening of SARS-CoV-2 inhibitors *via* ratiometric fluorescence of RBD–ACE2 complexes in living cells by competitive binding



## KEY WORDS

SARS-CoV-2;  
RBD–ACE2 interaction;  
Inhibitors screening;  
Live-cell imaging

## To the Editor:

The current coronavirus disease-19 (COVID-19) pandemic spurs the development of antiviral drugs for SARS-CoV-2, as the number of patients with viral infections continues to rise globally in the context of widespread vaccination. Targeting the interaction between the receptor binding domain (RBD) of SARS-CoV-2 spike protein and the host cell ACE2 is a promising therapeutic strategy to effectively inhibit viral entry, because the strong binding between RBD and ACE2 is the first step of viral infection<sup>1</sup>. Screening in live cells, represented by live or pseudo virus assays, have been approved to significantly improve effectiveness of the obtained inhibitors<sup>2,3</sup>. However, they are greatly limited by the biosafety level 3 facilities or multistep experimental procedures. Therefore, the development of rapid cell-based screening methods under virus-free conditions are still urgent needs for effective RAB inhibitors discovery.

Self-labeling protein tags (such as SNAP-tag and Halo-tag) can site-specifically label small molecule fluorescent dyes, which were widely used for live-cell proteins imaging to monitor protein–protein interactions<sup>4,5</sup>. Herein, we developed SNAP-fused ACE2 and Halo-fused SARS-CoV-2 RBD which were labeled with organic dyes, respectively, for RBD–ACE2 binding (RAB) inhibitors screening in living cells (Fig. 1). The proof-of-concept protein–protein disruption was demonstrated using wild ACE2, RBD, spike protein, and commercial RBD neutralizing

antibody (RBD-NAb) as ACE2 or RBD competitive inhibitors. Combined with virtual screening, this assay identified a small molecule inhibitor. The role of this small molecule with RBD was further verified by pseudo-typing and live virus infection test and molecular dynamics simulations.

## 1. Design of RBD/ACE2 fusion protein with self-labeling tag

We fused Halo-tag to C-terminal of truncated RBD R319–F541 residues, obtaining RBD (319–541)-halo (R541H). Meanwhile, SNAP-tag was fused to the N terminal of ACE2, obtaining SNAP-ACE2 (SA) (Fig. 1B, Supporting Information Table S1). R541H displayed high activity detected by ELISA assay (Supporting Information Fig. S1A). The live-cell screening process was shown in Fig. 1A, SA-overexpressed live cells were single labeled with SNAP-Cy3 (Fig. 1B, referred to as SA-Cy3). We can monitor RAB by imaging the ratiometric fluorescence after the addition of Halo-SiR (Fig. 1B) labeled RBD (referred to as R541H-SiR). The ratiometric signal was made by a combination of SA-Cy3 as a reference fluorophore (no change in signal upon analyte's presence) and the R541H-SiR as a dynamic fluorophore (decrease in signal upon analyte's presence), which permitted the quantification of analyte. When RAB were disrupted by ACE2 or RBD inhibitors, decreased RBD/ACE2 (R/A) ratiometric fluorescence on the cell membrane was obtained owing to the competing binding of inhibitors to RBD/ACE2.

## 2. Establishment and validation of live-cell RAB inhibitors screening assay

A co-localization imaging between SA-Cy3 and R541H-SiR was observed on the cell surface while R541H-SiR cannot stain the cells without expressing SA. And RBD-NAb blocking RAB was observed by the decrease of R541H-SiR fluorescence from cell

Peer review under responsibility of Chinese Pharmaceutical Association and Institute of Materia Medica, Chinese Academy of Medical Sciences

<https://doi.org/10.1016/j.apsb.2022.05.033>

2211-3835 © 2022 Chinese Pharmaceutical Association and Institute of Materia Medica, Chinese Academy of Medical Sciences. Production and hosting by Elsevier B.V. This is an open access article under the CC BY-NC-ND license (<http://creativecommons.org/licenses/by-nc-nd/4.0/>).

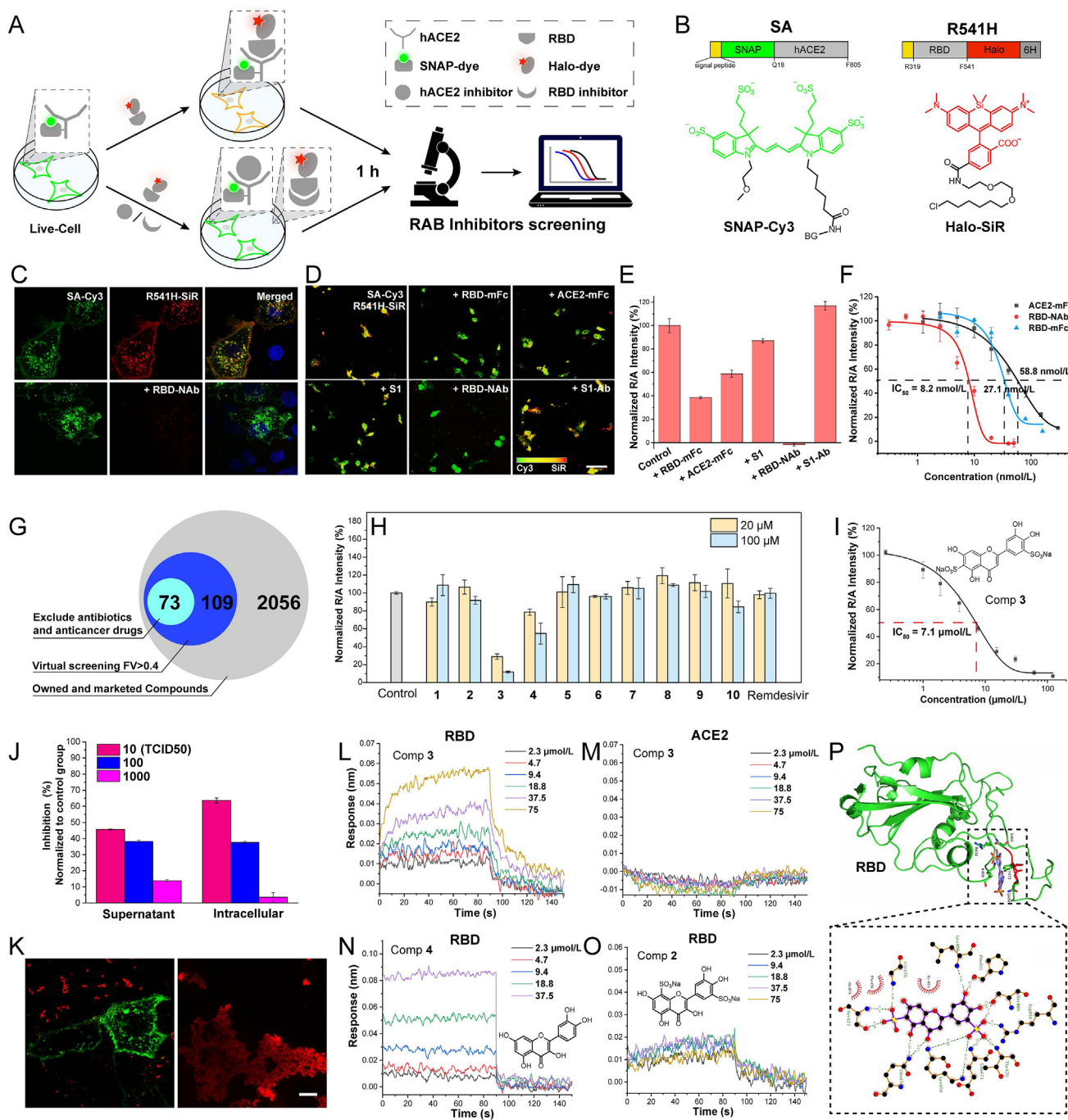


**Figure 1** Rapid screening of SARS-CoV-2 RAB inhibitors in living cells *via* ratiometric fluorescence imaging. (A) Schematic representation of live-cell screening strategy for RAB inhibitors. (B) Plasmid constructs of fusion protein and chemical structures of SNAP/Halo dyes. (C) Fluorescence imaging of HeLa/SA cells treated with SNAP-Cy3, R541H-SiR, and Hoechst 33342 without or with the addition of RBD-NAb. Scale bar: 10  $\mu\text{m}$ . (D) Fluorescence imaging of live HeLa/SA-Cy3 treated with the pre-incubated mixtures of R541H-SiR (25 nmol/L) and various protein-based inhibitors (40 nmol/L). Scale bar: 100  $\mu\text{m}$ . The colour bar representing the visual ratio change between Cy3 (green) and SiR (red). (E) The normalized R/A intensity of various protein-based inhibitors in (D). (F) Dose–response analysis of ACE2-mFc, RBD-NAb and RBD-mFc as RAB inhibitors. (G) Hit summary from owned and marketed compounds. (H) Screening of small molecule inhibitors with LCAR-RFI assay. (I) Dose–response analysis of compound **3**, showing  $\text{IC}_{50}$  value and compound **3** structure. (J) SARS-CoV-2 infection analysis of compound **3** (100  $\mu\text{mol/L}$ ). (K) Fluorescence imaging of LCAR-RFI system stained with 120  $\mu\text{mol/L}$  compound **3**. The R541H-SiR aggregation was observed in the solution. Scale bar: 10  $\mu\text{m}$ . (L–O) BLI sensorgram showing binding of compound **3** to RBD (L) and ACE2 (M), and the binding of compound **4** (N) and compound **2** (O) to RBD. (P) Snapshot of the primary binding pose of compound **3** (purple stick) to RBD (green cartoon). Enlarged dotted box was Ligplus plots of the surrounding residues burying the compound **3** molecule at the primary binding pose.

surface (Fig. 1C). The activity of R541H were tested in living cells by collecting the R/A ratiometric fluorescence at different RBD concentrations ( $EC_{50} = 25$  nmol/L, Fig. S1B), indicating both R541H and SA displayed high activity. And then live cells/SA-dye/R541H-dye ratiometric fluorescence imaging (LCAR-RFI) system was established to screen RAB inhibitors. This system can be used for different fluorescent channel and cell line requirement (Fig. S1C). Subsequently, commercial ACE2-mFc and RBD-NAb as RBD inhibitors, SARS-CoV-2 wild RBD-mFc and S1 as ACE2 inhibitors, and a S1 normal antibody (S1-Ab, without neutralizing performance) were tested to determine the practicality of LCAR-RFI assay (Fig. 1D, E). RBD-NAb showed the highest inhibition efficiency while S1-Ab cannot block the binding of R541H to SA at all. And the inhibition efficiency of RBD-mFc was higher than S1, which is consistent with the ELISA assay data reported by the vendor ( $EC_{50}$  of RBD-mFc and S1 to ACE2 were 0.3–1 and 2.6–7.8 nmol/L, respectively). The dose–response analysis indicated that RBD-NAb, ACE2-mFc, and RBD-mFc harboured discernible dose-dependent inhibitor activities (Fig. 1F), the  $IC_{50}$  of which were 8.2, 58.8, and 27.1 nmol/L, respectively. It indicated the capability of the system to screen SARS-CoV-2 RAB inhibitors quantitatively.

### 3. Small molecule screening by LCAR-RFI assay

We employed the system for RAB inhibitor screening with small molecule compounds. To this end, a manually-built pharmacophore model was used for virtual screening of 2056 molecules, which included 143 molecules in our lab and 1913 drugs recorded in Pharmaceutical Substances of Thieme Chemistry (Fig. 1G). Along with remdesivir, 8 of the 73 compounds were selected to be evaluated with LCAR-RFI assay at 20 and 100  $\mu$ mol/L (Fig. 1H, Supporting Information Fig. S2). Simultaneously, quercetin (compound 4) with Fitvalue 0.376 and iso-orientin (compound 7) with Fitvalue of 0.297 were tested, considering their structural feature. The structures of compounds 1–10 were shown in Supporting Information Scheme S1. Encouragingly, both compounds 3 and 4 displayed inhibitory effects. Compound 3 showed 72% inhibition at 20  $\mu$ mol/L while compound 4 was only 21%.

The concentration-dependent fluorescence imaging of compound 3 displayed differential ratiometric changes on the cell surface (Supporting Information Fig. S3). And the fluorescence change was resulted from the competing binding of compound 3 to RBD/ACE2, since compound 3 cannot influence the fluorescence intensity of SiR-labeled Halo protein in DMEM solution (Supporting Information Figs. S4A and B). In addition, compound 3 showed no cytotoxicity to Hela cells even at the concentration of 1 mmol/L (Fig. S4C), which might be due to poor cell membrane penetration of the high water-soluble compound resulting from the two sulfonic groups in the structure. The dose–response analysis converted from fluorescent imaging displayed that the  $IC_{50}$  value of compound 3 was 7.1  $\mu$ mol/L (Fig. 1I). The inhibitory effect of it was confirmed by pseudovirus assay, where the  $IC_{50}$  value was detected to be 41.7  $\mu$ mol/L (Fig. S4D). We further investigated the ability of compound 3 to inhibit virus infection by pre-incubating it with live SARS-CoV-2 and then infecting to Vero E6 cells. 100  $\mu$ mol/L compound 3 inhibited 45% (supernatant) and 60% (intracellular) of virus replication at 10 TCID<sub>50</sub> (Fig. 1J). The inhibition was existed even when the TCID<sub>50</sub> was increased to 1000.

### 4. Binding of RBD by the inhibitor prevents its entry into the cell

We observed the aggregation of R541H-SiR outside the cells and the fluorescence of it in solution was reduced when incubated with high concentration of compound 3, while compound 3 did not aggregate Halo proteins (Fig. 1K, Figs. S4A and B). And similar but smaller aggregations were observed in solutions of cells incubated with compounds 2 and 4 (Fig. S2). It indicated that compounds 2–4 inhibit RAB by binding to RBD. This conjecture was confirmed by bio-layer interferometry (BLI) experiment. The strong binding of compound 3 to RBD ( $K_D = 8.37$   $\mu$ mol/L) was observed, while it almost did not bind to ACE2 (Fig. 1L, M). Meanwhile,  $K_D$  of compound 4 to RBD was measured to be 75.6  $\mu$ mol/L, and compound 2 showed weak binding to RBD (Fig. 1N, O). These results were consistent with above LCAR-RFI tests. Although the binding affinity between compound 3 and RBD is only on the micromole level, a large amount of compound 3 can precipitate the RBD protein after blocking RAB to achieve the inhibitory effect. In addition, membrane impermeability of the compound made it almost non-toxic to cells ( $IC_{50} > 1$  mmol/L). Thus, it can be used in large quantities in living cells to inhibit virus entry.

In order to further understand the binding mechanism of compound 3 on the RBD, all-atom molecular dynamics (MD) simulations with well-tempered metadynamics were used to explore the possible binding sites of compound 3 on the RBD. Our metadynamic simulations indicated that primary binding site to compound 3 of RBD was found underneath the RBD S469–S477 loop region (Fig. 1P). The positively charged R454 and K458 firmly interact with the sulfonate ground of compound 3 to trap the compound and extensive hydrogen bonding interactions were observed between compound 3 and the RBD S469–S477 loop, which would inhibit the conformational variations of this region and, thus, block the RAB. The work reported by Xu et al.<sup>6</sup> have demonstrated that the RBD T470–T478 loop of SARS-CoV-2 spike is a crucial region for specific recognition of SARS-CoV-2 RBD by ACE2.

In summary, we engineered a live-cell ratiometric fluorescence imaging strategy to rapid screen virus entry inhibitors. By fusing Halo/SNAP tag to RBD and ACE2, organic dyes were covalently self-labelled to RBD and ACE2 for ratiometric fluorescence imaging RAB on the cell surface. A small molecule inhibitor, compound 3, with  $IC_{50}$  value of 7.1  $\mu$ mol/L was screened out. Our ongoing studies apply this strategy to screen inhibitors of mutant SARS-CoV-2 including Delta and Omicron, hope to deal with viral pandemic.

### Acknowledgments

This work is supported by the National Natural Science Foundation of China (22078314, 21878286, 21908216) and Dalian Institute of Chemical Physics (DICPI202142, DICPI202006, DICPI201938, DICPZZBS201805, China).

### Author contributions

Concepts were conceived by Zhaochao Xu and Lu Miao; Lu Miao designed the experiments and analyzed the data; Lu Miao, Chunyu Yan, Xuelian Zhou and Yingzhu Chen performed live cells experiments; Wei Zhou, Qinglong Qiao and Guangying Wang performed compounds synthesis; Zhendong Guo, Jun Liu and Hailong Piao performed antiviral assays; Yuebin Zhang and Guohui Li performed MD simulation Xia Pan, Mengxue Yan, Weijie Zhao and Yueqing Li

performed virtual screening of pharmacophore model; Lu Miao, Yuebin Zhang, Yueqing Li and Zhaochao Xu wrote the manuscript.

### Conflicts of interest

The authors declare no competing interests.

### Appendix A. Supporting information

Supporting data to this article can be found online at <https://doi.org/10.1016/j.apsb.2022.05.033>.

### References

1. Lan J, Ge J, Yu J, Shan S, Zhou H, Fan S, et al. Structure of the SARS-CoV-2 spike receptor-binding domain bound to the ACE2 receptor. *Nature* 2020;**581**:215–20.
2. Riva L, Yuan S, Yin X, Martin-Sancho L, Matsunaga N, Pache L, et al. Discovery of SARS-CoV-2 antiviral drugs through large-scale compound repurposing. *Nature* 2020;**586**:113–9.
3. Nie J, Li Q, Wu J, Zhao C, Hao H, Liu H, et al. Quantification of SARS-CoV-2 neutralizing antibody by a pseudotyped virus-based assay. *Nat Protoc* 2020;**15**:3699–715.
4. Gautier A, Juillerat A, Heinis C, Correa Jr IR, Kindermann M, Beauflis F, et al. An engineered protein tag for multiprotein labeling in living cells. *Chem Biol* 2008;**15**:128–36.
5. Los GV, Encell LP, McDougall MG, Hartzell DD, Karassina N, Zimprich C, et al. HaloTag: a novel protein labeling technology for cell imaging and protein analysis. *ACS Chem Biol* 2008;**3**:373–82.
6. Xu C, Wang Y, Liu C, Zhang C, Han W, Hong X, et al. Conformational dynamics of SARS-CoV-2 trimeric spike glycoprotein in complex with receptor ACE2 revealed by cryo-EM. *Sci Adv* 2021;**7**:eabe5575.

Lu Miao<sup>a,†</sup>, Wei Zhou<sup>a,†</sup>, Chunyu Yan<sup>a</sup>, Yuebin Zhang<sup>c</sup>, Qinglong Qiao<sup>a</sup>, Xuelian Zhou<sup>a</sup>, Yingzhu Chen<sup>a</sup>, Guangying Wang<sup>a</sup>, Zhen-dong Guo<sup>d</sup>, Jun Liu<sup>d</sup>, Hailong Piao<sup>a</sup>, Xia Pan<sup>b</sup>, Mengxue Yan<sup>b</sup>, Weijie Zhao<sup>b</sup>, Guohui Li<sup>c,\*</sup>, Yueqing Li<sup>b,\*</sup>, Zhaochao Xu<sup>a,\*</sup>,

<sup>a</sup>CAS Key Laboratory of Separation Science for Analytical Chemistry, Dalian Institute of Chemical Physics, Chinese Academy of Sciences, Dalian 116023, China

<sup>b</sup>State Key Laboratory of Fine Chemicals, Department of Pharmaceutical Sciences, School of Chemical Engineering, Dalian University of Technology, Dalian 116024, China

<sup>c</sup>State Key Laboratory of Molecular Reaction Dynamics, Dalian Institute of Chemical Physics, Chinese Academy of Sciences, Dalian 116023, China

<sup>d</sup>Institute of Military Veterinary Science, The Academy of Military Medical Science of PLA, Changchun 130000, China

\*Corresponding authors.

E-mail addresses: zcxu@dicp.ac.cn (Zhaochao Xu); yueqingli@dlut.edu.cn (Yueqing Li); ghli@dicp.ac.cn (Guohui Li).

Received 22 May 2022

Revised 31 May 2022

Accepted 31 May 2022

<sup>†</sup>These authors made equal contributions to this work.